Proceedings of the International Conference on Industrial Engineering and Operations Management

Publisher: IEOM Society International, USA DOI: 10.46254/BA08.20250390
Published: December 20, 2025

Optimizing Performance of Novel ITO/LBSO/$FASnI_3$/CuO Perovskite Solar Cell: Role of Defect and Interface Engineering Via SCAPS 1D

Md. Fardous Hasan Bappy, Abdullah-Al-Mazed Khan, Arnika Tabassum Arni and Md. Saiful Islam Shanto
Materials Science and Engineering Department
Rajshahi University of Engineering and Technology, Rajshahi, Bangladesh
fardousbappy23@gmail.com, abdullah.khan@mse.ruet.ac.bd, tabassum.arnika210@gmail.com, mdsaifulislamshanto01@gmail.com

Abstract

One of the most widely discussed solar cells lately is the perovskite solar cell, due to its high PCE, adjustable bandgap, and low-cost. Conversely, the intrinsic and interfacial defect densities may potently affect the stability and functionality of these cells since they act as recombination centers and restrict the carrier transport extremely. This paper gives a numerical performance analysis of a lead-free perovskite solar cell (ITO/LBSO/$FASnI_3$/CuO) structure via SCAPS-1D software. The $FASnI_3$ was chosen as absorber material because of its desirable band gap and non-toxicity, whereas LBSO and CuO were used as the electron and hole transport layers, respectively, owing to their desirable energy level alignment. We examine the effects of the density of defects in the absorber layer, the transport layers, and the variations in the absorber thickness. According to our results, the drastic enhancements in final PCE, from 19.20 % to 29.46 %, can be achieved by adjusting bulk defect densities to the range of $1x10^{-17}$ to $1x10^{-13}$. Better performance occurs during optimization of absorber thickness up to 1000 nm. These observations underline the ability to manipulate the level of defects and thickness to design and develop stable and efficient PSCs technologies.

Keywords
Perovskite, Deep-level defect, Interface, Recombination loss, SCAPS 1D

1. Introduction

The perovskite solar cells (PSCs) have entered fierce competition with potential high efficiency in performance as well as cost-effective manufacturing technology combined with attractive optoelectronic properties. Perovskite itself is the most simple ABX_3- type structure, with A being predominantly a relatively small cation of organic or inorganic materials, such as (FA^+), (MA^+), or (Cs^+); B is a bivalent metal cation like lead (Pb^+); and X is an anion halide, such as I^-, Br^-, or Cl^- (Dale and Scarpulla 2023). Efficiency in laboratory demonstrations has surpassed 24.2% for PSCs Xiang et al. (2021), coming very close to the commercial maximum performances of silicon solar cells 26.7% (Jena et al. 2019). Indeed, large scale and low-cost applications for mass production are possible using fabrication techniques such as inkjet printing, slot-die coating, and blade coating which critically cut down capital expenses. However, unintentional charge defect incorporation during low-temperature crystallization happens almost always in the microcrystalline halide perovskite (HP) layers (Heo et al. 2017). Such defects are usually caused by anion vacancies at the X site, interstitial cations at the A/B-site, or by degradation products such as metallic Pb^0, free FA^+/MA^+ or even volatile by-products like HI and I_2 (Moia and Maier 2021). The specific A-site cations and structural arrangements of BX_6 octahedra seriously affect perovskites' stability and electrical characteristics (Nowsherwan et al. 2021). $FAPbI_3$ is one of the most thoroughly studied composition in perovskites due to its bandgap of 1.45~1.51 eV and its simple phase transition (Shin et al. 2017). Illuminating mixed-halide $FAPbI_{1-x}Cl_x$ will only make them undergo phase segregation that will result in voltage losses and a lower uniformity of devices (Hoke et al. 2015). Defects in HP films

create shallow states, e.g., iodine vacancies, or deep-level states, such as free FA^+ or interstitials that provide a trap for carriers and recombination sites (Green et al. 2014). Deep-level trap states, which are located near the mid-bandgap, have a much worse impact on device performance than shallow states, whose positions are near the conduction or valence band edges (Green et al. 2014). Their existence promotes non-radiative recombination and severely constrains V_{OC} and Gt PCE. These types of states have been described by the use of multiple diagnostic methods which include time-resolved photoluminescence (TRPL), deep-level transient spectroscopy (DLTS) and transient photocurrent methods. According to Danladi et al. (2023), traps ~0.65 and ~0.76 eV below the conduction band have their origins from iodine anti-site and A-cation vacancies, respectively, and they drastically alter carrier lifetimes and recombination dynamics. Energy loss in organic-inorganic halide perovskite solar cells is mainly attributed to structural defects (e.g. creation of vacancies and interstitial positions) within the crystalline lattice and loss by non-radiative annihilation of carriers at grain boundaries and surface areas. The theoretical research on the defect physics of such hybrid systems is so numerous so as to determine why the energy dissipation and poor V_{OC} occur in such structures due to the presence of the trap states. Perovskite solar cells are not suitable for outdoor application over extended periods because they lack stability. This has prompted recent efforts in defect passivation, interface engineering, and compositional tuning to address these challenges. SCAPS-1D simulations become very powerful tools in assessing the defect density effects, particularly on defects in the perovskite bulk and interfacial regions (n/i and p/i interfaces) (Vlk et al. 2025).

Despite the great informational value of the results obtained through simulation studies, there is an experimental lack of research on $FASnI_3$-based PSCs because researchers still have not been able to overcome the instability of materials and fast oxidation of $Sn^{2+}$to Sn^{4+}. Recent experimental reports demonstrate that achieving stable, high-efficiency $FASnI_3$ devices requires precise control over processing conditions and defect passivation strategies. For example, Galve-Lahoz et al. (2024) achieved 9.66% PCE and strong air stability in $FASnI_3$ cells via organic additive passivation, Meng et al. (2020) achieved a stabilized PCE of 10.16% with controlled crystal growth and passivation additives, Kayesh et al. (2025) achieved ≈12% PCE in $FASnI_3$ cells using 2PTU additive for defect passivation. Despite these advances, reported experimental PCE values for $FASnI_3$ cells generally may remain below 15%, with significant challenges in reproducibility and long-term operation under ambient conditions. This highlights a critical gap between experimental performance and theoretical potential.

The current research work intends to analyse the role of deep level defect density on performance for $FASnI_3$-based PSC structured as ITO/LBSO/$FASnI_3$/CuO/Au in a p-i-n structure to study V_{OC}, J_{SC}, FF and PCE, as the major device performance parameters. The varying densities of the defects were made systematically in simulation studies and how these trap states influenced recombination, charge transport and total efficiencies are found out through analysis. Such results will be beneficial for defect engineering strategies that will ultimately contribute to efficiency improvement and long-term operational stability in lead-free PSC designs.

2. Device Structure and Methodology

SCAPS-1D is several simulation tools that are used to solve the electrical behaviour of semiconductor cells. The tool was developed at the University of Ghent, Belgium. Solving Poisson and continuity equations for electrons and holes is the basis of an understanding in depth understanding concerning charge transport, recombination mechanisms and photoconversion efficiencies under various operating conditions. The study involved utilization of SCAPS-1D to investigate how defect densities affect the performance of ITO/LBSO/$FASnI_3$/CuO perovskite solar cells. Each

layer's band energy and the overall structure is shown in (fig 1). By then analysing these critical output metrics including Voc, Jsc, FF, and PCE, it was possible to systematically vary defect densities in various relevant layers of the device. SCAPS-1D functions by simulating carrier dynamics through the drift-diffusion framework that governs carrier dynamics through fundamental semiconductor equations (De Sarkar and Ghosh 2024). Poisson's equation determines the spatial variation of electric potential within the device:

$$\frac{d^2V}{dx^2} = -\frac{q}{\varepsilon}(p + n + N_D^+ - N_A^-) \qquad (1)$$

Where V refers the electrostatic potential, ε as the
material's permittivity, q refers the elementary charge, n and p represent electron concentrations and hole concentrations, and N_D^+ denotes donor densities and N_A^- correspond to acceptor densities (Yıldırım 2008). Charge transport follows the charge continuity principles for both electrons and holes:

$$\frac{dJ_n}{dx} = q(G - R) \quad (2)$$

$$\frac{dJ_p}{dx} = -q(G - R) \quad (3)$$

where J_n and J_p are the electron current density and hole current density respectively, G represents the rate of charge generation, and R denotes the rate of recombination (Coropceanu et al. 2007). Carrier movement in the device is derived by the current density equations, which take into account both drift and diffusion mechanisms:

$$J_n = qn\mu_n E + qD_n \frac{dn}{dx} \quad (4)$$

$$J_p = qp\mu_p E - qD_p \frac{dp}{dx} \quad (5)$$

where μ_n and μ_p are the electron mobility and hole mobility respectively, D_n and D_p are their respective coefficient of diffusion, and *E* is the electric field (Marshak and Van Vliet 1984). These equations enable SCAPS-1D to simulate charge carrier movement, recombination, and extraction efficiency under different defect conditions. La-doped $BaSnO_3$ (LBSO) has many advantages over regular electron transport layers like SnO_2, TiO_2, ZnO, and CdS-latest developments for promising spin-offs for perovskite solar cells (PSCs) (Rabhi et al. 2024). One of them is the superior electron mobility that leads to more efficient charge transport and recombination losses, resulting in improved efficiency of the devices, compared to SnO_2 (Hossain et al. 2022). The photostability of LBSO is also better when compared to that of TiO_2, which is popularly known for its photocatalytic activity in UV light and therefore tends to degrade over time the perovskite layer (Samiul Islam et al. 2021). Another important aspect of LBSO is the reduced chemistry with perovskite materials, which is not the same with ZnO, as it can react with perovskite absorbers and produce adverse by-products that harm the stability of the devices (Marimuthu et al. 2023).

Moreover, LBSO is an alternative material to CdS because the toxicity of it's products would be eliminated; thus, it does not contain toxic heavy metals like this cadmium, which bear significant health and environmental risks (Akinpelu et al. 2018). All these qualities make LBSO the alternative epitaxial layer of choice by which efficiency, stability, and sustainability in perovskite solar cell technology improve. For the sake of HTL, CuO surpasses any standard organic HTL like Spiro-OMeTAD and PEDOT: PSS because it has high stability and excellent properties of hole conduction. For instance, unlike Spiro-OMeTAD, which is moisture-and-temperature variation sensitive, CuO is quite strong environmentally when it comes to long-term use in solar cells. This means that with its wider band gap compared to Spiro-OMeTAD, it would be able to extract the holes efficiently while minimizing recombination losses (Golshani et al. 2022). Its earth abundance and cost-effective material resources make CuO a highly promising material for large-scale solar cells production. An extensive variation of bulk defect density was considered for the simulation, from a low of 1×10^{13} cm^{-3} and up to a maximum of 1×10^{17}, to clarify the influence exerted on charge recombination and carrier transport. In contrast, the two distinct values of interface defect density were analysed for the purpose of quantifying the effect of interfacial recombination on efficiency; these two values are at the extremes for this simulation setup: high (1×10^{16} cm^{-3}), low (1×10^{13} cm^{-3}). The simulations were done under standard AM 1.5G solar illumination at 300 K (room temperature) while keeping the work function of the contacts at 4.7 eV for ITO and 5.1 eV for Au to facilitate charge extraction (Talbi et al. 2022).

Other parameters of used materials required for simulation are listed in Table 1. Utilizing these, a clear identification of the optimum defect's scenario with a minimum recombination loss will be ascertained for improved perovskite solar cell efficiency.

This methodology has offered an in-depth understanding of the way bulk and interface defects affect charge transport and photovoltaic performance through simulation of SCAPS-1D. The meticulous selection of CuO as the HTL and LBSO as the ETL ensures a proper balance between efficiency, stability, and environmental sustainability, along with the use of a lead-free $FASnI_3$ absorber (Wu et al. 2022). These have implications for further commercialization advancement in perovskite solar cells by addressing significant challenges related to defect passivation,charge transport optimization, and stability of the materials (Table 1 and Figure 1).

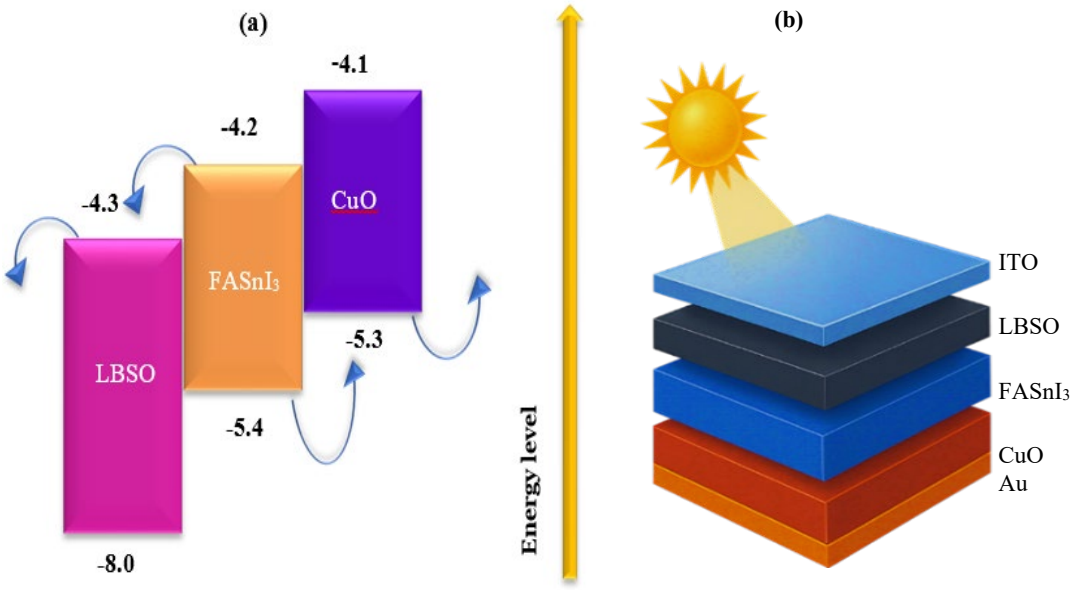

Figure 1. (a)Energy level of ETL, AL, HTL (b) Proposed device structure

Table 1. Structure (ITO/LBSO/$FASnI_3$/CuO) based on typical values from the literature

Properties	ITO	LBSO (ETL)	$FASnI_3$ (Absorber)	CuO (HTL)
Thickness (nm)	50	100	600*	100
Bandgap, E_g (eV)	3.5	3.12	1.41	1.5
Electron affinity, χ_e (eV)	4.0	4.4	4.2	4.07
Dielectric permittivity, ε_r	9	22	25	18.1
CB effective state density, N_C (cm^{-3})	2.2×10^{18}	1.8×10^{20}	1×10^{18}	2×10^{18}
VB effective state density, N_V (cm^{-3})	1.8×10^{19}	1.8×10^{20}	1×10^{18}	1.8×10^{19}
Thermal velocity of electron (cms^{-1})	1×10^{7}	1×10^{7}	1×10^{7}	1×10^{7}
Thermal velocity of hole (cms^{-1})	1×10^{7}	1×10^{7}	1×10^{7}	1×10^{7}
Mobility of electron (cm^2/Vs)	20	0.69	22	10
Mobility of hole (cm^2/Vs)	10	0.69	22	0.1
Shallow uniform donor concentration, N_D (cm^{-3})	1×10^{18}	2×10^{21}	0	0

Properties	ITO	LBSO (ETL)	$FASnI_3$ (Absorber)	CuO (HTL)
Shallow uniform acceptor concentration, N_A (cm^{-3})	0	0	1×10^{16}	1.38×10^{18}
Defect density, N_t (cm^{-3})	$1\times10^{14*}$	$1\times10^{14*}$	$1\times10^{14*}$	$1\times10^{14*}$
References	(Hossain et al. 2021)	(Shivesh et al. 2022)	(Alqurashi 2024), (Yasin et al. 2021)	(Ahmmed et al. 2021), (Daoudi et al. 2024)

3. Results and Discussion

3.1 Influence of Bulk Defect Density

The bulk density of defects strongly governs the performance of the device pertaining to PCE, FF, and V_{OC}. The defect density increasing from 1×10^{13} cm^{-3} to 1×10^{17} cm^{-3} would enhance recombination losses leading to the efficiency drop. At a thickness of 200 nm, this would correspond to a shift in PCE from 22.63% to 16.72%, while at 1000 nm absorption thickness, the PCE is much higher at 25.79%. This means that thick absorbers are favourable for the purpose of defect loss mitigation. In the same manner, at maximum defect density, the falling charge transport renders the FF to decrease from 85.45% down to 78.56%. The V_{OC} dropped from 0.992 V to 0.906 V, while J_{SC} was almost constant, indicating bulk defects affect carrier collection more than generation. These results are shown in (Fig 2).

3.2 Effect of Interface Defect Density

Interface defect density is significantly reduced, which dramatically increases performance. Under this extremely low defect density (1×10^{13}), the PCE rises to 29.42%, particularly for thicker absorbers. The FF also raises to 88.1%, indicating better extraction of charges, shown in (Fig 3). An improvement also observed in V_{OC}, which moves from 0.992 V to 1.087 V, confirming less optimism to recombination due to the interfaces. J_{SC} remains stable, supporting even more the fact that the charge transport improved mainly through interface passivation and not generation. These observations manifest the criticality of interface optimization for improving the overall efficiency concerning defect passivation for its necessary high-performance.

3.3 Combined Impact of Bulk and Interface Defects

A comparative analysis of the two types of defects reveals that while the bulk defects mostly affect the PCE, the interface defects are essential for V_{OC} and FF consideration. Even when both defects are high, PCE still remains lower than 26%; reducing the interface defects, however, is expected to improve it to near 30% at optimal thickness, shown in Fig.3. The optimal thickness is found to be 900-1000 nm, with both bulk and interface defects reduced, which further shows that passivating the interface is more important for improving efficiency. Optimal defect management would provide the best results on perovskite solar cells by ensuring effective charge transport while minimizing losses (Figure 2 and Figure 3).

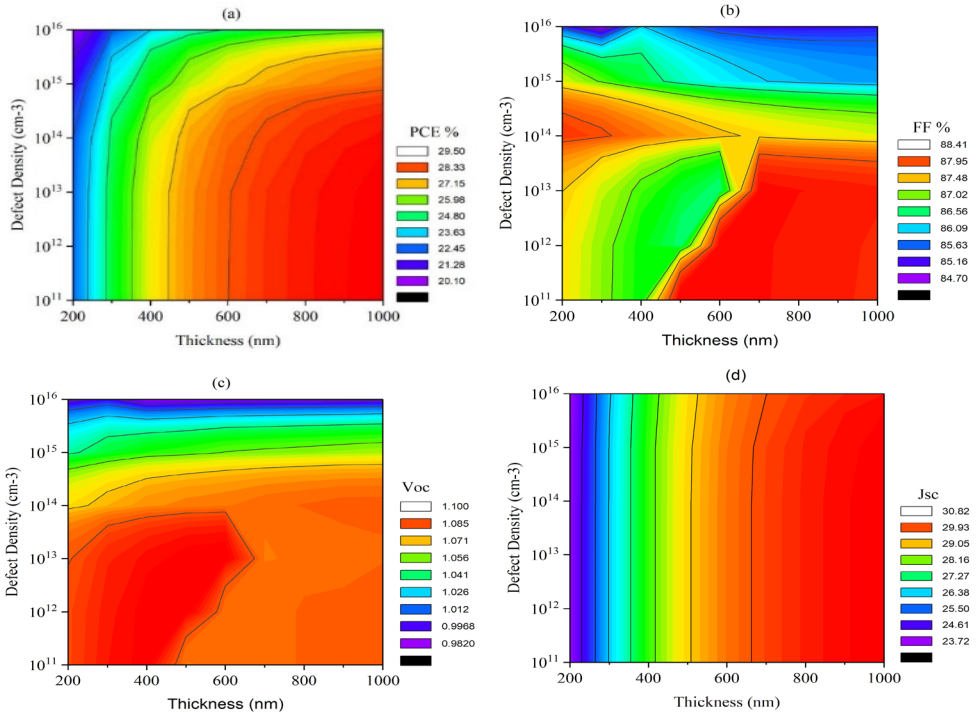

Figure 2. Bulk defect density in (ETL, AL, HTL) layers and effects on (a)PCE (b) FF (c) Voc (d) Jsc.

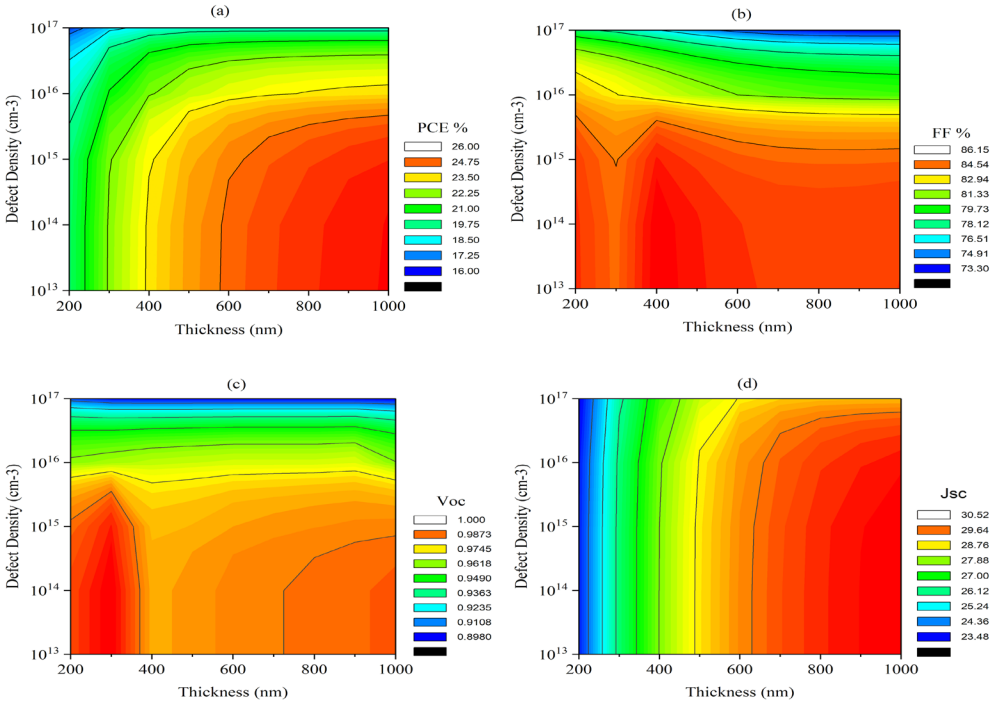

Figure 3. Interface defect density in (ETL, AL, HTL) layers and effects on (a)PCE (b) FF (c) Voc (d) Jsc.

3.4 Sensitivity Analysis

Device performance showed clear sensitivity to variations in defect densities and absorber thickness. Increasing bulk defect density reduced PCE from 25.79% to 16.72%, while lower interface defect density improved PCE up to 29.42% and VOC to 1.087 V. Thicker absorbers (900–1000 nm) mitigated recombination losses, while JSC remained stable across all conditions. These trends confirm that defect passivation and optimized layer thickness are key for achieving high-performance $FASnI_3$ solar cells

3.5 J-V Characteristic Curve Analysis

The J-V (current density-voltage) curve is a very useful plot that shows the good and bad effects of defect engineering on the solar cell's main output parameters. In Fig.4. the black line represents the baseline device and shows the lowest performance, which is characterized by the lowest open-circuit voltage(V_{OC}) of around 0.9 V and the most rounded "knee," thus indicating a poor fill factor (FF). The red line symbolizes a reduction in bulk defects, which leads to a tremendous performance increase; the V_{OC} rises to almost 1.0 V, and the curve turns to be very "squarer," which is a sign of a higher FF. Lastly, the device with both bulk and interface defects reduced (blue line) obtains the best performance. It shows the highest V_{OC} (more than 1.1 V) and the highest FF. The plot very convincingly supports the conclusions drawn from the sensitivity analysis, as it shows that the short-circuit current (J_{SC}) stays more or less the same, but the V_O and FF improve a lot just by reducing the bulk and, especially, the interface defects (Figure 4).

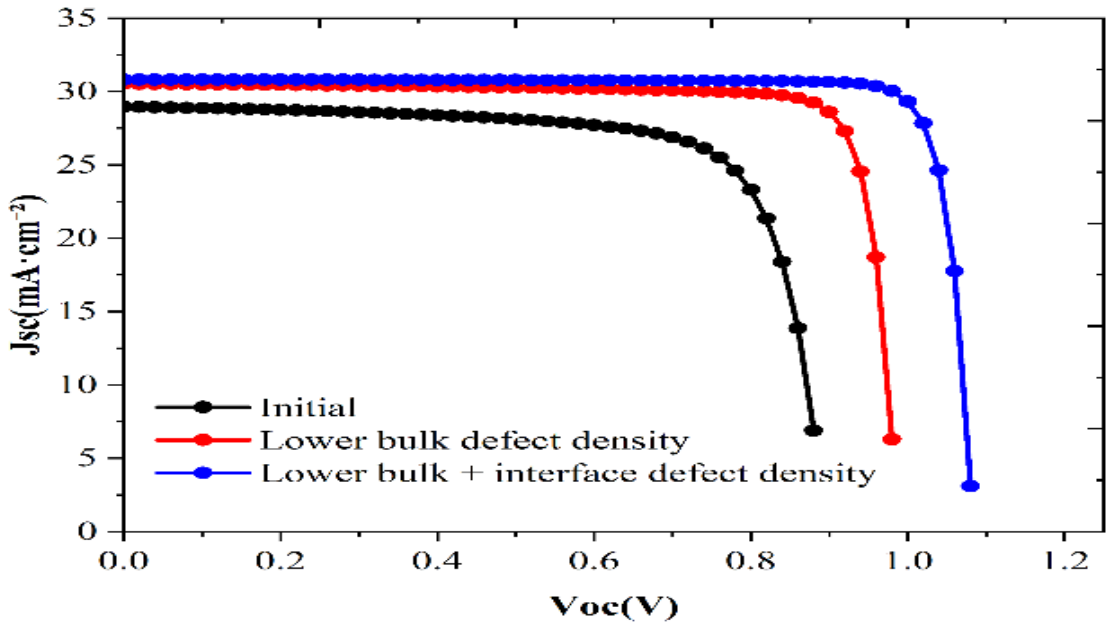

Figure 4. J-V (current density-voltage) characteristic curves showing the impact of defect engineering.

4. Conclusion

Defect density and grain size are particularly the most defining variables of the $FASnI_3$ perovskite solar cell efficiency. Bulk defects cause larger recombination loss and have a negative impact on Voc, FF, and PCE, and interface defects cause larger charge extraction that has beneficial impacts on device performance. At 900-1000 nm of absorber thickness, the most favorable efficiencies were observed, as here fewer bulk and interface defects existed. Such findings emphasize the significance of dealing with the strategies of defect passivation to achieve PSC maximum efficiency. However, there are still a couple of difficult obstacles. Future research should be focused on the creation of efficient passivation that would not only enhance the tolerance of defects but also the environmental stability of the substance. The future development of other ways of deposition and new methods of doping could be the solution to using this technology on a large scale. Therefore, the requirement of examining the other compositional variations and doping plans to extend carrier lifetime and cut recombination losses in these conditions. Whether all these challenges will be overcome will determine the success of transferring high-performing lab-scale PSCs to the development of commercially viable solar ready to be deployed on a large scale.

References

Ahmmed, S., Aktar, A. and Ismail, A. B. Md., Role of a Solution-Processed V2O5 Hole Extracting Layer on the Performance of CuO-ZnO-Based Solar Cells, *ACS Omega*, vol. 6, no. 19, pp. 12631–12639, 2021.

Akinpelu, A., Akinojo, O. A., Usikalu, M. R., Onumejor, C. A. and Arijaje, T. E., A Numerical Simulation and Modeling of Poisson Equation for Solar Cell in 2 Dimensions, *IOP Conference Series: Earth and Environmental Science*, vol. 173, pp. 012001, 2018.

Alqurashi, R. S., Comprehensive investigation of material properties and operational parameters for enhancing performance and stability of FASnI3-based perovskite solar cells, *Scientific Reports*, vol. 14, no. 1, pp. 16511, 2024.

Coropceanu, V., Cornil, J., da Silva Filho, D. A., Olivier, Y., Silbey, R. and Brédas, J.-L., Charge Transport in Organic Semiconductors, *Chemical Reviews*, vol. 107, no. 4, pp. 926–952, 2007.

Dale, P. J. and Scarpulla, M. A., Efficiency versus effort: A better way to compare best photovoltaic research cell efficiencies?, *Solar Energy Materials and Solar Cells*, vol. 251, pp. 112097, 2023.

Danladi, E. et al., Defect and doping concentration study with series and shunt resistance influence on graphene modified perovskite solar cell: A numerical investigation in SCAPS-1D framework, *Journal of the Indian Chemical Society*, vol. 100, no. 5, pp. 101001, 2023.

Daoudi, O. et al., The outcomes of Zn doping on the properties of CuO thin films prepared via modified SILAR method and its impact on the performance of CuO-based solar cells using Cd0.4Zn0.6S-ETL and Spiro-OMeTAD-HTL, *Journal of Materials Science: Materials in Electronics*, vol. 35, no. 19, pp. 1353, 2024.

De Sarkar, P. and Ghosh, K. K., SCAPS-1D, *Advances in Microelectronics, Embedded Systems and IoT: Proceedings of 8th International Conference on Microelectronics, Electromagnetics and Telecommunications (ICMEET 2023)*, pp. 197, 2024.

Galve-Lahoz, S. et al., Addressing ambient stability challenges in pure FASnI3 perovskite solar cells through organic additive engineering, *Journal of Materials Chemistry A*, vol. 12, no. 33, pp. 21933–21943, 2024.

Golshani, Z., Maghsoudi, S. and Hosseini, S. M. A., Enhancement of the photovoltaic performance of HTL-free-perovskite solar cells based on carbon electrode via the modification of electron transport layer with Copper oxide@Polyaniline nanocomposite, *Energy Reports*, vol. 8, pp. 13596–13609, 2022.

Green, M. A., Ho-Baillie, A. and Snaith, H. J., The emergence of perovskite solar cells, *Nature Photonics*, vol. 8, no. 7, pp. 506–514, 2014.

Heo, S. et al., Deep level trapped defect analysis in CH3NH3PbI3 perovskite solar cells by deep level transient spectroscopy, *Energy & Environmental Science*, vol. 10, no. 5, pp. 1128–1133, 2017.

Hoke, E. T., Slotcavage, D. J., Dohner, E. R., Bowring, A. R., Karunadasa, H. I. and McGehee, M. D., Reversible photo-induced trap formation in mixed-halide hybrid perovskites for photovoltaics, *Chemical Science*, vol. 6, no. 1, pp. 613–617, 2015.

Hossain, M. I. et al., Perovskite/perovskite planar tandem solar cells: A comprehensive guideline for reaching energy conversion efficiency beyond 30%, *Nano Energy*, vol. 79, 2021.

Hossain, M. K., Rubel, M. H. K., Toki, G. F. I., Alam, I., Rahman, Md. F. and Bencherif, H., Effect of Various Electron and Hole Transport Layers on the Performance of CsPbI3-Based Perovskite Solar Cells: A Numerical Investigation in DFT, SCAPS-1D, and wxAMPS Frameworks, *ACS Omega*, vol. 7, no. 47, pp. 43210–43230, 2022.

Jena, A. K., Kulkarni, A. and Miyasaka, T., Halide Perovskite Photovoltaics: Background, Status, and Future Prospects, *Chemical Reviews*, vol. 119, no. 5, pp. 3036–3103, 2019.

Kayesh, M. E. et al., Optimization of Crystal Growth and Defect Passivation of FASnI3 Film by Using 2-Pyridylthiourea for Sn-Based Perovskite Solar Cells, *ACS Applied Energy Materials*, vol. 8, no. 4, pp. 2043–2049, 2025.

Marimuthu, S. et al., Drift diffusion modelling of cell parameters effect on the performance of perovskite solar cells with MXene as additives, *Solar Energy*, vol. 262, pp. 111804, 2023.

Marshak, A. H. and Van Vliet, C. M., Electrical current and carrier density in degenerate materials with nonuniform band structure, *Proceedings of the IEEE*, vol. 72, no. 2, pp. 148–164, 1984.

Meng, X. et al., Surface-Controlled Oriented Growth of FASnI3 Crystals for Efficient Lead-free Perovskite Solar Cells, *Joule*, vol. 4, no. 4, pp. 902–912, 2020.

Moia, D. and Maier, J., Ion Transport, Defect Chemistry, and the Device Physics of Hybrid Perovskite Solar Cells, *ACS Energy Letters*, vol. 6, no. 4, pp. 1566–1576, 2021.

Nowsherwan, G. A., Jahangir, K., Usman, Y., Saleem, W. and Khalid, M., Numerical modeling and optimization of perovskite silicon tandem solar cell using SCAPS-1D, *Scholars Bulletin*, vol. 7, pp. 171–184, 2021.

Rabhi, S. et al., Experimental findings and SCAPS-1D simulations for high-efficiency MAPbI3 perovskite solar cells beyond 31%, *Optical and Quantum Electronics*, vol. 56, no. 8, pp. 1372, 2024.

Samiul Islam, M. et al., Defect study and modelling of SnX3-based perovskite solar cells with SCAPS-1D, *Nanomaterials*, vol. 11, no. 5, pp. 1218, 2021.

Shin, S. S. et al., Colloidally prepared La-doped BaSnO3 electrodes for efficient, photostable perovskite solar cells, *Science*, vol. 356, no. 6334, pp. 167–171, 2017.

Shivesh, K., Alam, I., Kushwaha, A. K., Kumar, M. and Singh, S. V., Investigating the theoretical performance of Cs2TiBr6-based perovskite solar cell with La-doped BaSnO3 and CuSbS2 as the charge transport layers, *International Journal of Energy Research*, vol. 46, no. 5, pp. 6045–6064, 2022.

Talbi, A., Khaaissa, Y., Nouneh, K., Mustapha Feddi, E. and El Haouari, M., Effects of temperature, thickness, electron density and defect density on ZnS based solar cells: SCAPS-1D simulation, *Materials Today: Proceedings*, vol. 66, pp. 116–121, 2022.

Vlk, A. et al., Improving Voc of Lead Halide Perovskites Solar Cells by Plasma Treatment, *Proceedings of the International Conference on Hybrid and Organic Photovoltaics (HOPV25)*, 2025.

Wu, T. et al., Heterogeneous FASnI3 Absorber with Enhanced Electric Field for High-Performance Lead-Free Perovskite Solar Cells, *Nano-Micro Letters*, vol. 14, no. 1, pp. 99, 2022.

Xiang, W., Liu, S. and Tress, W., A review on the stability of inorganic metal halide perovskites: challenges and opportunities for stable solar cells, *Energy & Environmental Science*, vol. 14, no. 4, pp. 2090–2113, 2021.

Yasin, S., Moustafa, M., Al Zoubi, T., Laouini, G. and Abu Waar, Z., High efficiency performance of eco-friendly C2N/FASnI3 double-absorber solar cell probed by numerical analysis, *Optical Materials*, vol. 122, pp. 111743, 2021.

Yıldırım, S., Exact and Numerical Solutions of Poisson Equation for Electrostatic Potential Problems, *Mathematical Problems in Engineering*, vol. 2008, no. 1, 2008